

good photoconductor along the crystal axis at 4.2°K. For both polarization directions of the incident light the spectral dependence of the photocurrent shows structure related to the spectral dependence of the optical properties, in particular to the highly polarized reflection edge at 2 eV. However, the photocurrent per absorbed power is roughly independent of the photon energy and persists at least down to photon energies of 0.6 eV. We thus conclude that the photoconductivity is only indirectly connected to the optical properties in the visible and near infrared region and that the light supplies the energy for the electrons to overcome the interruptions in the conducting strands. Further details will be published in a forthcoming paper.

One might object that ionic conduction in the compound is conceivable, since the crystal structure is rather open and only a fraction of the potassium and bromine sites are occupied.² Furthermore, the compound was reported to decay under the action of an electric current.² We have passed a total charge of 2 A h through a crystal of $0.6 \times 0.4 \times 8$ mm³ size (i.e., about 10^3 elementary charges per atom) and did not find any significant change in the electrical resistance nor visual appearance of the crystal. We believe that the effect reported in Ref. 2 was thermal. Ionic conductivity would lead to electrolytic effects at much smaller charges, and

we may safely assume that the dc conductivity is electronic.

In conclusion we have shown that $K_2Pt(CN)_4Br_{0.3} \cdot (H_2O)_n$ has a one-dimensional metallic conductivity in the 10^{14} -Hz region. This is the first direct evidence for metallic behavior in a square planar organic-complex compound. The dc and low-frequency conductivity and the photoconductivity at low temperature can be understood in terms of a simple model assuming metallic strands interrupted by lattice defects.

We should like to acknowledge valuable discussions with Dr. S. Strässler, J. Bernasconi, and in particular Dr. C. Schüller who drew our attention to this material. Thanks are also due to A. Beck, J. Dlouhy, and W. Hinz for technical assistance.

¹For a review see K. Krogmann, *Angew. Chem., Int. Ed. Engl.* **8**, 35 (1969).

²K. Krogmann and H.-D. Hausen, *Z. Anorg. Allg. Chem.* **358**, 67 (1968).

³S. B. Piepho, P. N. Schatz, and A. J. McCaffery, *J. Amer. Chem. Soc.* **91**, 5994 (1969).

⁴A. S. Berenblyum, L. I. Buravov, M. D. Khidekel', I. F. Shchegolev, and E. B. Yakimov, *Pis'ma Zh. Eksp. Teor. Fiz.* **13**, 619 (1971) [*JETP Lett.* **13**, 440 (1971)].

⁵A. V. Sokolov, *Optical Properties of Metals* (Blackie and Son, London and Glasgow, 1967).

⁶M. J. Minot and J. H. Perlstein, *Phys. Rev. Lett.* **26**, 371 (1971).

Acoustic Paramagnetic Resonance in a Dense Magnetic Insulator

J. G. Miller,* Peter A. Fedders,* and D. I. Boleff†

Arthur Holly Compton Laboratory of Physics, Washington University, Saint Louis, Missouri 63130

(Received 27 August 1971)

The first observation of acoustic paramagnetic resonance in a dense magnetic system (RbMnF₃) is reported and a theory proposed which correctly predicts the shape of the observed line.

We report the observation of acoustic paramagnetic resonance (APR) in a dense magnetic insulator and propose a theory, valid in the high-temperature limit ($T \gg T_N$), which correctly predicts the shape of the observed APR line. The experiment was carried out at 293 K utilizing 1.1-GHz longitudinal phonons propagated along the [110] axis of a single crystal of the dense cubic paramagnet RbMnF₃. RbMnF₃ becomes antiferromagnetic at $T_N = 82$ K. The acoustic absorption as a function of magnetic field exhibits a characteristic square-root shape and includes contributions from both positive and negative frequencies.

Although electron paramagnetic resonance studies are routinely carried out in both dilute and dense paramagnetic systems, APR has been observed heretofore only in dilute magnetic systems.^{1,2} Theoretical estimates of APR in dense paramagnetic systems such as RbMnF₃ have been previously made.^{2,3} Such dense magnetic systems are characterized by strong dipole-dipole coupling and large exchange forces. Since both dipolar and exchange forces are strongly dependent upon interatomic distance, a periodic lattice vibration resulting from the propagation of an ultrasonic wave might be expected to induce

transitions in the spin system. In Ref. 2 an order-of-magnitude estimate of $3 \times 10^{-2} \text{ cm}^{-1}$ for the strength of the APR absorption due to dipolar coupling for a typical dense magnetic insulator (MnF_2) at 300 K and 1 GHz was proposed for an assumed linewidth of 0.3 kOe (1 GHz). Estimates from moment calculations, however, suggest that a linewidth of 300 kOe (10^3 GHz) is more appropriate.²⁻³ Calculations⁴ made by one of us (P.A.F.) indicate that the linewidth should actually lie between these two extremes.

A typical APR absorption line at $T = 293$ K and 1.1 GHz is shown in Fig. 1(a). The single-crystal specimen of RbMnF_3 was that used by Melcher and Bolef.⁵ The data of Fig. 1(a) were taken with the magnetic field rotated in the $(1\bar{1}0)$ plane by an angle θ of 30° from the $[110]$ direction of propagation. The data were taken with a conventional ultrasonic pulse-echo spectrometer utilizing a multichannel analyzer for signal averaging. Changes in acoustic absorption were measured by means of a precision attenuator. To

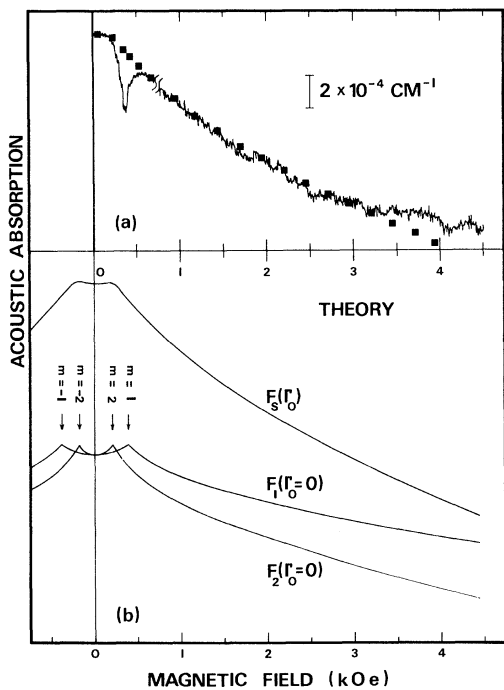


FIG. 1. Acoustic absorption as a function of magnetic field H_0 . (a) Recorder tracing for 1.1-GHz longitudinal waves, $\vec{q} \parallel [110]$ with \vec{H} at $\theta = 30^\circ$ from \vec{q} in $(1\bar{1}0)$ plane, in the TbMnF_3 specimen. $T = 293$ K. The squares represent the theoretical $F_s(\Gamma_0)$ curve of (b). The narrow line centered at $g=2$ is the electromagnetically induced EPR line instrumentally superimposed for calibration purposes. (b) Plots of F_m [Eq. 2] with $\Gamma_0=0$, and of F_s with $\Gamma_0=58$ Oe.

achieve better resolution at low fields, the data of Fig. 1(a) were taken in two runs, one from 0 to 0.75 kOe, the other from 0.75 to 4.5 kOe. The solid squares are taken from the $F_s(\Gamma_0)$ theoretical curve of Fig. 1(b). The APR curve in Fig. 1(a) is characterized by a broad maximum extending from 0 to approximately 0.5 kOe, followed by a slow decrease in amplitude to 4.5 kOe, the maximum field applied. The difference in ultrasonic absorption between $H_0=0$ and 4.5 kOe is $1.3 \times 10^{-3} \text{ cm}^{-1}$. The narrow "dip" [centered at $g=2$ in Fig. 1(a)] is the electromagnetically induced EPR line, which was instrumentally superimposed on the broad APR absorption and was utilized to calibrate the APR line in magnitude and field. Measurements of the dependence of the APR absorption on θ indicated the presence of an angle-independent contribution, consistent with the theoretical predictions for $m = \pm 1$ and $m = \pm 2$ transitions, to be discussed below.

Data on the APR absorption taken at 150 K indicate an order-of-magnitude increase in absorption over that observed at room temperature. The 150-K data exhibit a sharper "peaking" at $H=0$ and an increased anisotropy in the angular dependence.

In contrast with our observations of APR, EPR absorption in dense magnetic insulators⁶⁻⁸ consists of an intense, narrow line occurring at the resonant frequency $\omega_0 = \gamma H_0$, where H_0 is the applied magnetic field and γ is the electronic gyro-magnetic ratio. The shape of the EPR line in RbMnF_3 , which is characteristic of a strongly exchange-coupled paramagnetic system, has been analyzed carefully.⁶ Our EPR results on the present specimen agree in all important respects with those previously reported.

The reason why EPR and APR experiments yield such different results is simply that, even at high temperatures, the Heisenberg paramagnet is a strongly interacting system and is therefore not equivalent to an equal number of noninteracting spins. Bandwidths due to spin-spin exchange interactions can be orders of magnitude larger, in fact, than typical Zeeman energies. In spite of these complications, some aspects of the system at low frequencies (ω much less than the exchange frequency) and long wavelengths ($qa \ll 1$, where $q = 2\pi/\lambda$ and a is an interatomic spacing), the region of interest in the present experiment, are well understood. In this limit and in the absence of any anisotropic spin-dependent forces or external magnetic fields, the dynamic susceptibility or two-spin correlation function is

dominated by spin diffusion.⁹ A generalization¹⁰ of the dynamic susceptibility to include external magnetic fields and small anisotropy forces is

$$\chi_m''(q, \omega) = \chi_0 \omega \Gamma(q) / [(\omega - m\omega_0)^2 + \Gamma^2(q)], \quad (1)$$

where $\Gamma(q) = \Gamma_0 + Dq^2$. This represents that part of the susceptibility tensor associated with transitions centered at $m = +1, 0$, and -1 , where χ_0 is the static susceptibility. Γ_0 is the intrinsic linewidth as measured in EPR experiments and D is the spin-diffusion coefficient.

Since the coupling of an electromagnetic field to the spins is *linear* in the spin operators, since the wavelength of electromagnetic radiation is very large, and since the total spin of the system commutes with the exchange interaction, the exchange bandwidth is relatively unimportant in EPR experiments. The exchange interaction

$$f_m = \text{const} - \{[(\omega - m\gamma H_0)^2 + (2\Gamma_0)^2]^{1/2} + 2\Gamma_0\}^{1/2}. \quad (2)$$

In Fig. 1(b) are plotted curves for F_1 and F_2 with $\Gamma_0 = 0$ and for $F_s = F_1 + F_2$ (appropriate to an angular-independent attenuation) with Γ_0 assumed to be 58 Oe.⁶ Agreement between the theoretical curve F_s and the experimentally observed APR line, as shown by the solid squares in Fig. 1(a), is good between 0 and 3.2 kOe. Lack of agreement at high fields may be attributed to (i) a breakdown in the theory because $m\gamma H_0$ is no longer much less than the exchange frequency and to (ii) poorer signal to noise because of the smaller slope at higher fields. The vertical scale of the theoretical curve was adjusted for the best fit; the theory contains no other adjustable parameters.

James C. Zesch assisted in data taking.

*Work supported in part by the U. S. Air Force Office of Scientific Research under Grant No. AFOSR-71-2004.

comes into play only through the narrowing of the relatively small dipolar interaction, producing the exchange-narrowed linewidth Γ_0 . Thus EPR absorption signals are proportional to $\chi_{+1}''(q, \omega)$ with q essentially equal to zero.

Spin-phonon couplings, on the other hand, are *quadratic* in the spin operators, and thus the ultrasonic attenuation is proportional to four-spin correlation functions. Approximating this by a product of two-spin correlation functions leads to convolutions of two $\chi''(q, \omega)$'s. Fortunately, that part of the frequency and wave-number integrals which contribute to the field-dependent attenuation is dominated by low frequencies and long wavelengths. For values of $|\omega - m\gamma H_0|$ much less than the exchange frequency one obtains⁴ field-dependent contributions to the ultrasonic attenuation proportional to $F_m = f_m + f_{-m}$, where

†Work supported in part by the National Science Foundation.

¹E. B. Tucker, in *Physical Acoustics*, edited by W. P. Mason (Academic, New York, 1966), Vol. 4A.

²S. A. Al'tshuler, B. I. Kochelaev, and A. M. Leushin, *Usp. Fiz. Nauk* **75**, 459 (1961) [*Sov. Phys. Usp.* **4**, 880 (1962)].

³R. Loudon, *Phys. Rev.* **119**, 919 (1960).

⁴P. A. Fedders, to be published.

⁵R. L. Melcher and D. I. Bolef, *Phys. Rev.* **178**, 864 (1969).

⁶J. E. Gulley, D. Hone, D. J. Scalapino, and B. G. Silbernagel, *Phys. Rev. B* **1**, 1020 (1970).

⁷J. F. Siebert, Ph. D. thesis, University of California (Berkeley), 1968 (unpublished).

⁸E. Toyota and K. Hirakawa, *J. Phys. Soc. Jap.* **30**, 692 (1971).

⁹L. Kadanoff and P. C. Martin, *Ann. Phys. (New York)* **24**, 419 (1963).

¹⁰P. A. Fedders, *Phys. Rev. B* **3**, 2352 (1971).